

ON THE NATURE OF SURFACE DEFECTS FOUND IN 2/0 N-DOPED 9-CELL CAVITIES*

A. Cano[†], A. Grassellino, D. Bafia, J. Lee, Z-H. Sung, T. Spina, M. Martinello, A. Romanenko
 Fermi National Accelerator Laboratory, Batavia, IL, USA

Abstract

In this contribution, we present a surface characterisation on the microstructure of 1.3 GHz 9-cell TESLA type SRF cavity, processed with 2/0 Nitrogen-doping surface treatment, to explain the premature quench phenomenon observed in cavities that were submitted to this treatment. The microstructure was characterised using secondary electron images and advanced metallurgical techniques such as EBSD in parallel with chemical information obtained from spectroscopic techniques. The most remarkable difference was observed in the ends-cavities (one and nine), which showed roughening on the surface, revealing a series of morphologies associated with Nb cubic phase. The cell-to-cell analysis also showed standard pits with different geometry and distribution, located in grains and grain boundaries. The surface defects found in the multicell suggest that during the electropolishing process, the parameters such as temperature (T), current (I) and time (t), shown deviation from the standard procedure, insufficient to generate a smooth surface without discarding the role of the impurities, N and O, that could have induced the growth of these features.

INTRODUCTION

Niobium is the material of choice for SRF technology used in particle accelerators. Under operation conditions, the RF penetration depth is about 100 nm. From this fact, the local chemical composition and structural defects in that near-surface region are relevant for the cavity's performance. Different cavity treatments have been evaluated in the past to improve the cavity quality factor (Q₀), among them the N-doping, which results in a significant increase in the value of Q₀. Since a decrease in the structural defects in the near-surface region results in a better cavity performance, in this study, we are evaluating a 9-cell cavity processed with 2/0 N-doping treatment, which shows an unexpected early quench.

EXPERIMENTAL STUDIES

Cavity Preparation

The samples under study were extracted from all cells of the Nb 9-cell cavity (CAV018) processed with 2/0 N-doping surface treatment. The process stages are shown in Fig. 1. In addition, the surface of the cut-out was examined as received, using an EBSD/SEM instrument and Laser Confocal Scanning Microscopy.

* This manuscript has been authored by Fermi Research Alliance, LLC under Contract No. DE-AC02-07CH11359 with the U.S. Department of Energy, Office of Science, Office of High Energy Physics
[†] acano@fnal.gov

The surface chemical composition of these cut-outs was evaluated from XPS spectra recorded with an ESCALAB 250Xi from Thermo-Fisher spectrometer equipped with an AlK α source.

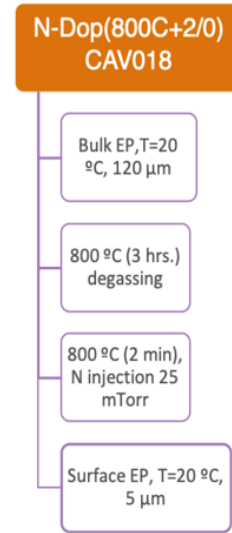


Figure 1: Process stages to evaluate the surface chemical composition.

RF Results

The 9-cell cavity shown an early quench during the RF test, locating the inducer region in cell 1, Fig. 2.

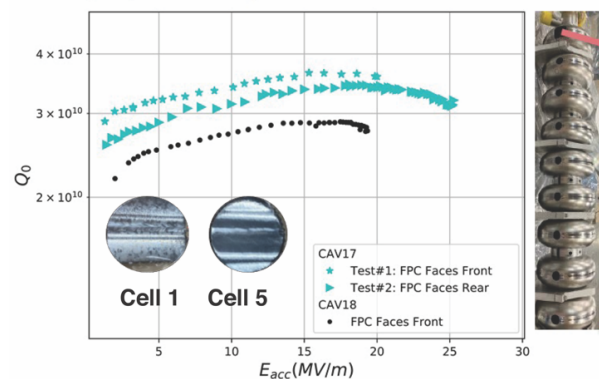


Figure 2: Q₀ vs E_{acc} curve of the 9-cell cavity (CAV018). The plot took from reference [1].

RESULTS AND DISCUSSION

Characterisation with XPS

XPS is a surface analysis technique that explores the near-surface region to a depth of about 7 nm using AlK(radiation)

and with a detection limit of >0.1 at %. Figure 3 shows typical survey XPS spectra for cells 1 and 9. These spectra reveal the presence of slight variation in the chemical composition of these two cells, mainly in C and O composition. As expected, their surface is formed by a homogeneous oxide layer, formed explicitly by Nb₂O₅, with a minor fraction of non-stoichiometric oxides. These last ones are probably located at the interface between the metal and the passivating Nb₂O₅ layer. In the recorded survey, XPS also appear peaks from species probably due to adsorbed contaminants, like hydrocarbons, Ca and Zn impurities. The SIMS profiles of C, N, and O discussed in detail elsewhere [1, 2] do not show any chemical composition variation in these elements from cell to cell and neighbouring grains. It seems the surface and in-depth (few microns) chemical compositions are not the cause that is inducing the early quench [3].

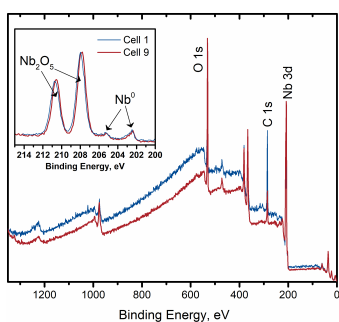


Figure 3: XPS survey spectra and high-resolution Nb 3d and O 1s recorded at four different points of the cutout extracted from cell #1. Residuals of Zn and Ca are found in all the analysed points from contaminants. The level of noise observed in the spectra indicates the scattering of the photoelectrons resulting from the differential surface topography.

Characterisation with Optical Microscopy

The optical images recorded from cell 1 show high contrast between neighbouring grains, related to irregular surface topography. We evaluated the surface roughness in cells 1, 5 and 9, resulting in average surface roughness from <0.10 μm (for mirror-like termination) to 0.90 μm (in etched grains). Except for cell 1, identified as the quench region inducer, we evaluated a three-grain junction, which shown significant differences in the average roughness (Ra) values, Fig. 4. We found that etched grains located only in cell 1 have the highest Ra values in the three-grain junction and the evaluated cells.

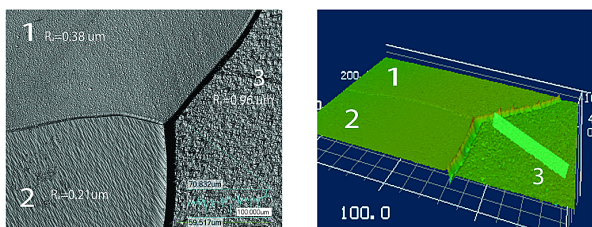


Figure 4: Optical image recorded with LCSM, and 3D map recorded from a three-grain junction from cell 1 showing significant differences in surface roughness.

Characterisation with SEM

All the samples extracted from each cell were evaluated via SEM electron microscopy for a microstructure study, Fig. 5.

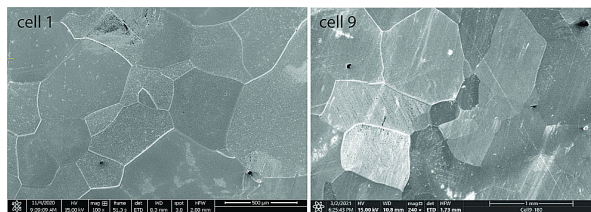


Figure 5: Surface of samples from (left) cell 1 and (right) cell 9. The samples were extracted from the area near the equatorial region.

In concordance with the optical images, few grains appear preferentially etched, revealing morphologies compatible with the cubic structure of metallic Nb, Fig. 6.

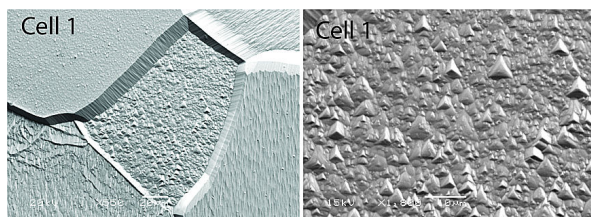


Figure 6: Morphologies observed in-grains: 1) small cubes with well-defined faces and edges, 2) stacked layer with a characteristic relief forming depressions of ellipsoidal shape along their transversal section, and 3) crystallites of irregular shape, probably related to chemical attack of the edges of small cubes during the electropolishing process.

The cell 1 to 8 were also evaluated (Fig. 7), and none of them shows preferential etching grains. On the other

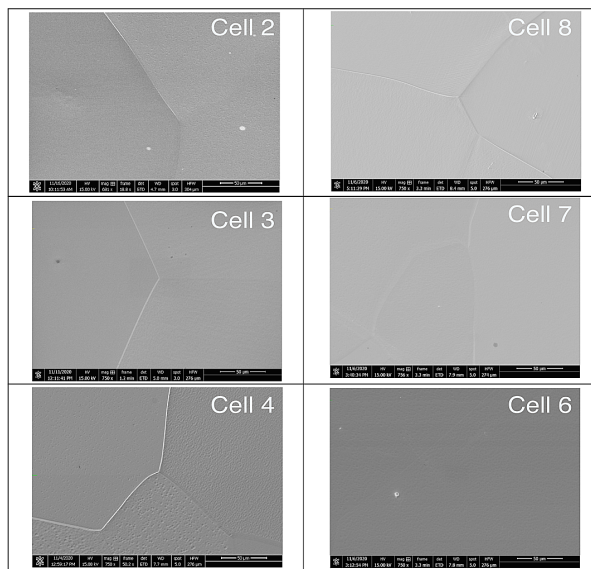


Figure 7: Surface morphology of 9-cell cavity processed with 2/0 N-doping surface treatment and submitted to material removal of 7 μm of standard T (21°C) electropolishing.

hand, the SEM images reveals that all the cavities shows pitting, that commonly occurs during the gas evolution stage resulted from increases on voltage, according to the current density-voltage curve of electropolishing [4]. The images recorded from cell-to-cell shown that these pits are located in-grain and grain boundaries, and differs in shape, size, and population.

Pitting was found in all the cells, together with the high roughness found in cell 1, which agrees with our statement that the final electropolishing applied to the 9-cell cavity differs from the standard process, and therefore insufficient to produce a mirror-like surface.

Characterisation with EBSD

To understand if the preferentially etched grains could have their origin in the grain orientation, EBSD maps were recorded from cells 1, 5 and 9, see Fig. 8. These maps corroborate that the grains with orientation (111), with a high density of atoms on the surface, are more sensitive to corrosion. This behaviour is observed in the EBSD maps recorded in cell 1. Nevertheless, the EBSD maps recorded from cell nine do not show this tendency.

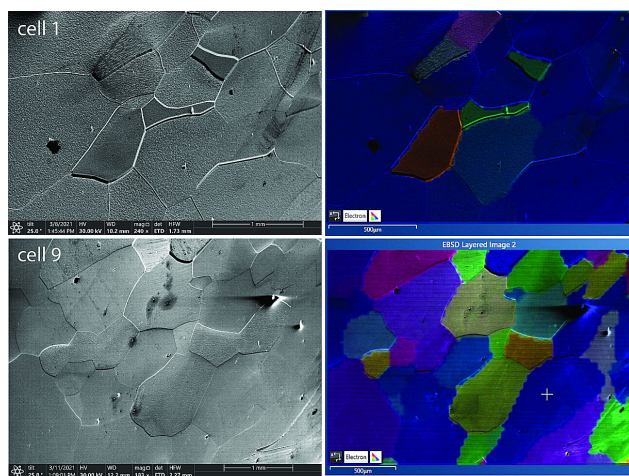


Figure 8: EBSD maps recorded from the cell 1 and 9. Colours are assigned to the grain orientation.

DISCUSSION

We have explored the surface topology, grain's structure, grain boundary, and the presence of surface irregularities that could be responsible for the unexpected early quenching observed in the Q_0 vs E_{acc} curve of the 9-cell cavity under study. According to the results herein discussed, such behaviour could be ascribed to insufficient removal of surface roughness during the electropolishing process. A surface topology well different from the mirror-like features was observed, quantified by the value of the Ra parameter. In the

cut-outs from these cells, this parameter takes values from 0.10 μm to 0.90 μm . The surface of cut-outs representative of cells 1 and 9 show a large population of crystals with pronounced corners typical of the crystal habits of Nb bcc, which were not removed. The appearance of such corners reveals that the electropolishing process was not optimised to produce a smooth structure. In addition, for some surface regions, pits of distant depths and sizes contribute to supporting such a hypothesis relative to an inappropriate surface polishing as a probable cause for the unexpected premature cavity quenching. Although supported in the above-discussed data, this hypothesis must be complemented with information regarding the potential effect of impurities in the Nb matrix on the material performance in the electropolishing process.

CONCLUSION

We have performed a systematic study of the microstructure in samples extracted from an N-doping 9-cell cavity. 1) Cells 1 and 9 show a high density of defects such as high-step grain boundaries, pits, and etched grains, which reveals morphologies with sharp edges; 2) The cell-to-cell evaluation shows the presence of defects such as pits in all the cells, which is not related to the removal of Nb-nitrides. The pits' role on the cell's performance needs to clarify; 3) In cell 1, a correlation was found between preferential grain attack with grain orientation on the (111) planes observed from EBSD maps. Further analysis will be carried out to understand the effect of the impurities on the appearance of these features.

ACKNOWLEDGEMENTS

The author(s) would like to thank A. Penhollow and D. Bice for the samples' preparation.

REFERENCES

- [1] D. Bafia *et al.*, "New insights in the quench mechanisms in nitrogen-doped cavities", in *Proc. 19th Int. Conf. on RF Superconductivity (SRF'19)*, Dresden, Germany, July 2019, pp. 592-596. doi:10.18429/JACoW-SRF2019-TUP062
- [2] A. Romanenko *et al.*, "First Direct Imaging and Profiling TOF-SIMS Studies on Cutouts from Cavities Prepared by State-of-the-Art Treatments", in *Proc. 19th Int. Conf. on RF Superconductivity (SRF'19)*, Dresden, Germany, July 2019, pp. 886-870. doi:10.18429/JACoW-SRF2019-THP014
- [3] C. Z. Antoine, "Influence of crystalline structure on rf dissipation in superconducting niobium", *Phys. Rev. Accelerators and Beams*, vol. 22, p.034801, March 2019. doi:10.1103/PhysRevAccelBeams.22.034801
- [4] W. Han and F. Fang, "Fundamental aspects and recent developments in electropolishing", *Int. J. Mach. Tools Manuf.*, vol. 139, p. 1-23, April 2019. doi:10.1016/j.ijmactools.2019.01.001